

1N-20  
3203  
15P

# Evaluation of Oxide-Coated Iridium-Rhenium Chambers

Brian D. Reed  
*Lewis Research Center*  
*Cleveland, Ohio*

Prepared for the  
1993 JANNAF Propulsion Meeting  
sponsored by the JANNAF Interagency Propulsion Committee  
Monterey, California, November 15-19, 1993



National Aeronautics and  
Space Administration

(NASA-TM-106442) EVALUATION OF  
OXIDE-COATED IRIIDIUM-RHENIUM  
CHAMBERS (NASA. Lewis Research  
Center) 15 p

N94-29097

Unc1as

G3/20 0003003

Trade names or manufacturers' names are used in this report for identification only. This usage does not constitute an official endorsement, either expressed or implied, by the National Aeronautics and Space Administration.

# TESTING AND EVALUATION OF OXIDE-COATED IRIIDIUM-RHENIUM CHAMBERS

Brian D. Reed  
National Aeronautics and Space Administration  
Lewis Research Center  
Cleveland, Ohio

## SUMMARY

Iridium-coated rhenium (Ir-Re) provides long life operation of radiation-cooled rockets at temperatures up to 2200 °C. Ceramic oxide coatings could be used to increase Ir-Re rocket lifetimes and allow operation in highly oxidizing environments. Ceramic oxide coatings promise to serve as both thermal and diffusion barriers for the iridium layer. Seven ceramic oxide-coated Ir-Re, 22-N rocket chambers were tested with gaseous hydrogen/gaseous oxygen ( $\text{GH}_2/\text{GO}_2$ ) propellants. Five chambers had thick (over 10 mils), monolithic coatings of either hafnia ( $\text{HfO}_2$ ) or zirconia ( $\text{ZrO}_2$ ). Two chambers had coatings with thicknesses less than 5 mils. One of these chambers had a thin-walled coating of  $\text{ZrO}_2$  infiltrated with sol gel  $\text{HfO}_2$ . The other chamber had a coating composed of an Ir-oxide composite. The purpose of this test program was to assess the ability of the oxide coatings to withstand the thermal shock of combustion initiation, adhere under repeated thermal cycling, and operate in aggressively oxidizing environments. All of the coatings survived the thermal shock of combustion and demonstrated operation at mixture ratios up to 11. Testing the Ir-oxide composite-coated chamber included over 29 min at mixture ratio 16. The thicker walled coatings provided the larger temperature drops across the oxide layer (up to 570 °C), but were susceptible to macrocracking and eventual chipping at a stress concentrator. The cracks apparently resealed during firing, under compression of the oxide layer. The thinner walled coatings did not experience the macrocracking and chipping of the chambers that was seen with the thick, monolithic coatings. However, burn-throughs in the throat region did occur in both of the thin-walled chambers at mixture ratios well above stoichiometric. The burn-throughs were probably the result of oxygen diffusion through the oxide coating that allowed the underlying Ir and Re layers to be oxidized. The results of this test program indicated that the thin-walled oxide coatings are better suited for repeated thermal cycling than the thick-walled coating, while thicker coatings may be required for operation in aggressively oxidizing environments.

## INTRODUCTION

The most common material system currently used for low thrust, radiation-cooled rockets is a niobium (Nb) alloy (C-103) with a fused silica coating (R-512A or R-512E) for oxidation protection. Significant amounts of fuel film cooling are usually required to keep the material below its maximum operating temperature of 1370 °C, however, which degrades engine performance. A new class of high-temperature, oxidation-resistant materials is under development for radiation-cooled rockets. These materials have the thermal margin to allow rocket operation up to 2200 °C, thereby reducing or eliminating fuel film cooling while still exceeding the life of silicide-coated Nb (refs. 1 and 2). The most developed of these high-temperature materials is iridium-coated rhenium (Ir-Re). A 22-N Ir-Re chamber was operated for 15 h at 2200 °C on monomethyl hydrazine (MMH) and nitrogen tetroxide (NTO) propellants with negligible internal erosion, while a flighttype 440-N chamber was successfully tested for 6.3 h on MMH/NTO (ref. 3). There has been further testing of flighttype 22-N, 62-N, and 440-N Ir-Re engines on MMH/NTO, and 22-N and 440-N engines on hydrazine nitrogen tetroxide ( $\text{N}_2\text{H}_4/\text{NTO}$ ) by various rocket companies (ref. 1). A 22-N Ir-Re chamber has also been tested for over 14 h on gaseous hydrogen/gaseous oxygen ( $\text{GH}_2/\text{GO}_2$ ) propellants at low mixture ratio.

The two known life-limiting mechanisms of Ir-Re rockets are shown in figure 1. It was found that Re slowly diffuses along grain boundaries into the Ir coating during high temperature operation, so that the concentration of Re at the inner wall surface slowly increases (ref. 4). Oxidation testing at 1540 °C showed that the Ir oxidation rate increases significantly with a Re concentration above 20 percent (ref. 3). Rhenium diffusion into Ir and oxidation of the resulting Ir-Re alloy was then identified as a major life limiting mechanism for Ir-Re rockets. Successful long life tests of Ir-Re rockets had been performed using a platinum liner or regeneratively cooled section in the near injector region of the chamber (ref. 3). In recent testing (refs. 1 and 5), erosion or pitting of the Ir coating has occurred, primarily in the head end region of the chamber. The reasons for the Ir degradation are not yet certain, although it appeared to occur only when the Ir was exposed to a still-mixing, still-combusting flow field. Iridium reactivity with combustion radicals or locally high concentrations of oxidizers are suspected causes for the Ir degradation. Degradation of the Ir coating threatens to be a more rapid life-limiting mechanism for Ir-Re rockets than the diffusion mechanism.

The addition of ceramic oxide coatings to Ir-Re rockets is being investigated as a way to increase the oxidation resistance and lifetime of Ir-Re rockets. The oxide coatings would serve both as a thermal barrier and as a diffusion barrier for the Ir coating, as shown in figure 2. The presence of an oxide coating (particularly a coating with a low thermal conductivity) would lower the temperature at the Ir-Re interface, and thus, decrease the temperature-dependent diffusion rate of Re into Ir. Though there would be some oxygen diffusion through the coating, the oxide coating would still significantly reduce the amount of oxidizers exposed to the Ir surface, lower the Ir surface temperature, and slow the Ir oxidation rate. The coating would also serve to retard the egress of Ir oxidation products. Furthermore, the addition of ceramic oxide coatings would prevent direct exposure of the Ir surface to the flow field. The oxide coatings, then, would serve as a protector against possible Ir reactivity with a mixing, combusting flowfield, and the slower diffusion life limiting mechanism would determine the chamber lifetime. The synergistic effects of ceramic oxide coatings could result in significantly longer life operation for Ir-Re rockets, even in more oxidizing environments, such as  $\text{GH}_2/\text{GO}_2$  at high mixture ratios.

The development of oxide coatings for Ir-Re rocket chambers was the subject of a Small Business Innovative Research (SBIR) contract (NAS3-25468; NAS3-26253) with Ultramet, funded by the Ballistic Missile Defense Organization (refs. 6 and 7). The primary coatings developed were  $\text{ZrO}_2$  and  $\text{HfO}_2$ . These refractory oxides have higher melting points than Ir, but are permeable to oxygen ( $\text{O}_2$ ) to some degree and therefore cannot be used as a primary oxidation barrier. The main technology issue associated with these oxide coatings is their ability to withstand the thermal shock of combustion and to adhere after several thermal cycles. Thermomechanical, thermochemical, and mass transport modeling of the oxide-iridium-rhenium material system was performed and is summarized in reference 8. Seven oxide-coated Ir-Re rocket chambers were fabricated under the SBIR contract. Fabrication and material analysis of these chambers are also discussed in reference 8. This paper will discuss the testing of the rocket chambers with  $\text{GH}_2/\text{GO}_2$  propellants, in nonoxidizing and severely oxidizing environments. The condition of the oxide coatings throughout and after testing will be described, and the temperature drop through the oxide layer and entire wall will be estimated.

## CHAMBERS

After reviewing and screening potential ceramic oxide coatings in Phase I of the SBIR contract (ref. 6),  $\text{ZrO}_2$  and  $\text{HfO}_2$  were selected for application to Ir-Re chambers. In Phase I of the SBIR contract, an Ir-Re chamber was fabricated with a 1-mil  $\text{ZrO}_2$  coating infiltrated with sol gel (a colloidal suspension)  $\text{HfO}_2$ . In Phase II of the program, six more chambers were fabricated. Five chambers had monolithic coatings of  $\text{ZrO}_2$  and  $\text{HfO}_2$  of thicknesses greater than 10 mils. The other chamber had a thin

layer of an Ir-oxide composite coating. The structures of the chambers, with the measured as-deposited thicknesses of the layers just before the beginning of the converging section, are summarized in table I.

The chamber geometry used in this study had been successfully fabricated by Ultramet and tested by Gencorp Aerojet in previous rocket chamber material screenings (ref. 3). The chamber design had a long barrel section, with a diameter of 0.894 cm, a length of 3.5 cm, and a characteristic length ( $L^*$ ) of 18.3 cm, to promote mixing and combustion. The contraction ratio was 4.3 with a smooth, gradual converging contour to the throat, which had a diameter of 0.432 cm. The nozzle was an 8:1 area ratio, 15°-half-angle cone. A 37°-angle cone at the head end was used for attachment to the injector assembly.

## TEST FACILITY

Testing of the chambers was conducted at a NASA Lewis Research Center propulsion test facility, Rocket Lab 11 (ref. 9). The facility was designed for research of low thrust rockets operating on  $\text{GH}_2/\text{GO}_2$  propellants, at thrust levels below 220 N, in long duration steady state or cyclic tests. The rocket was mounted in a 0.91-m, cylindrical test tank with viewports for optical access. A two-stage air ejector system maintained a 1.4-kPa pressure in the tank, equivalent to an altitude of 36.6 km. The rocket axis was oriented horizontally in the thrust stand and was mounted on flexible plates to insure freedom of movement along the thrust axis. The rocket was fired into a water-cooled diffuser, where the exhaust was cooled by water spray, prior to entering the air ejectors and venting through mufflers. All data were recorded on a PC-based data acquisition system, and performance parameters were calculated in real time during testing. A more detailed description of the test facility is available in reference 9.

## TEST APPARATUS

### Injector Assembly

The chambers were attached to an assembly consisting of a water-cooled section and an injector. The injector body had a center annulus for a spark plug. The  $\text{O}_2$  was injected radially around the spark plug tip to flow down the center annulus. A small amount of hydrogen ( $\text{H}_2$ ) was injected radially downstream of the spark plug to ignite the energized  $\text{O}_2$ . Six impinging elements injected  $\text{H}_2$  into the center annulus flow, while six elements of the same size as the impinging elements injected  $\text{H}_2$  axially into the chamber. The 5.08-cm-long water-cooled section had a trip ring 2.54 cm downstream of the injector face, to promote mixing of the flow and to smooth out any stratifications. The water-cooled section also protected the front end from thermal soakback from the chamber. The water flow rate through the section was typically 7.6 L/min. The conical head end of the chamber was attached to a cone on the water-cooled section face. The chamber was clamped to the water-cooled section by a split ring and sealed with 0.0127- and 0.0254-cm sheets of grafoil, a flexible graphite gasket material.

### Purge Assembly

Since testing was performed in high altitude air, the exterior Re surface was purged with an inert gas to prevent the oxidation of the Re and an “outside-in” failure of the chamber. No exterior purge would be necessary in the space operation of these chambers. A 24-element ring was used for injection of the purge gas around the chamber exterior. The purge was contained in a 5.20-cm diameter fused silica tube, with a 2.54-cm inner diameter, stainless steel end cap. Springs were used to hold the tube to the purge ring, while allowing some movement due to thermal growth. Argon was used initially as a purge gas at a flow rate of 67 scfh. Because of availability, helium was used later in testing, initially at a

100-scfh flow rate and finally at a flow rate of 150 scfh. An  $O_2$  absorbing purifier was used in the purge line to insure that the purge gas had less than 0.1 parts/million of  $O_2$ . The purge was for the most part successful in preventing the oxidation of the exterior Re. The exit plane of the nozzle was positioned just outside of the tube to avoid recirculation of the plume back into the tube. However, there were incidents during thruster shutdown when the facility back pressure would increase and briefly wash the plume back into the tube. Also, the exterior Re at the nozzle exit was susceptible to oxidation from both the air in the test tank and the hot oxidizers in the plume. There also was some oxidation of the exterior Re at the head end, since there was a small portion of the chamber that sat behind the purge ring injection point.

## Instrumentation

A pressure tap in the injector behind the combustion zone was used to measure the static chamber pressure. This chamber pressure measurement was corrected for pressure drop across the flame front (due to momentum loss) and converted to total pressure. Hydrogen and  $O_2$  mass flow rates were calculated from the measured inlet pressures, the measured inlet temperatures, and the discharge coefficients of critical flow venturis with corrections for real gas effects (ref. 10). The measurement uncertainties of the mass flow rates and mixture ratio were determined using the Joint Army, Navy, NASA, Air Force (JANNAF) recommended procedure (ref. 11). The measurement uncertainties were less than  $\pm 0.5$  percent for all of the mass flow rates and  $\pm 0.6$  percent for the mixture ratio.

The outer wall temperature of the chamber was measured with an Ircon Modline Plus two-color pyrometer. The two-color pyrometer viewed two wavelength bands (one ranging from 0.7 to 1.08  $\mu m$  and a narrow band centered at 1.08  $\mu m$ ) and used the ratio of the two signals to calculate temperature. As such, the absolute emissivity of the target was not required, but rather, the change in emissivity over the two wavelength bands. For the black, dendritic Re surfaces in this testing, the emissivity was assumed to be constant over the two wavelength bands. The two-color pyrometer was aimed at the beginning of the converging section on the chamber (the position of highest temperature) and had an approximately 1.0-cm diameter spot size. The temperature range of the two-color pyrometer was from 980 to 3315  $^{\circ}C$ , and the uncertainty in the temperature measurements was estimated to be  $\pm 27^{\circ}C$ .

## TEST PROGRAM

### Test Matrix

Although MMH/NTO and  $N_2H_4$ /NTO propellants are more commonly used for low thrust propulsion systems, testing with the more energetic  $GH_2/GO_2$  combination is useful in evaluating the life and compatibility of chamber materials. The mole fraction of  $O_2$  as a function of mixture ratio was calculated by the Chemical Equilibrium Composition code (ref. 12) (assuming complete combustion). The mole fractions of  $O_2$  for mixture ratios 4 and 4.5  $GH_2/GO_2$  are at the same low levels as for the MMH/NTO and  $N_2H_4$ /NTO propellant combinations, respectively, at their optimum mixture ratios. Above mixture ratio 5, however, the  $O_2$  mole fraction for  $GH_2/GO_2$  begins to increase significantly. At mixture ratios above 8 (stoichiometric), the  $O_2$  mole fractions for  $GH_2/GO_2$  are two orders of magnitude higher than for the storable propellant combinations.

In this program, the chambers were exposed to a well-mixed, well-combusted flow of  $GH_2/GO_2$ . The nominal test matrix began with a 5-s duration and five 15-s duration tests at mixture ratio 4. This testing was performed to determine the ability of the coating to withstand the thermal shock of combustion initiation in a nonoxidizing environment. Testing was then performed at mixture ratios of 6

and 8, which increased both the temperature and amount of  $O_2$  of the flow field. At each of these mixture ratios, a 5-, 15-, and 300-s duration test was performed. At mixture ratio 8, two additional 300-s tests were conducted. All seven chambers survived the initial testing intact, so a series of ten 60-s duration tests was performed at mixture ratio 11 for six of the chambers. The high mixture ratio testing determined the ability of the coating to operate in an aggressively oxidizing environment. The composite-coated chamber was tested for 60-s durations at mixture ratios of 10, 12, and 14, and the balance of the testing was done at mixture ratio 16. The interest in testing at mixture ratio 16 resulted from a recommended operating point in a  $GH_2/GO_2$  reaction control system for future reusable, manned launch vehicles (ref.13).

The majority of testing occurred at chamber pressures from 572 to 627 kPa. When a test was shut down before the end of its planned duration, the balance of the time was made up in another test. Frequent visual inspections of the chambers were made during the testing. The test results for each chamber are summarized in table II.

### Wall Temperature Profile

The inner wall temperatures of the chambers were estimated by using an energy balance between the one-dimensional, steady state heat conduction through the chamber wall and the radiation emitted from the chamber outer wall, as shown in figure 3. The inner wall temperature can be determined in terms of the radii of the layers, the thermal conductivities of the layers, the outer wall emissivity, the ambient temperature, and the external wall temperature. The temperatures at the oxide-Ir and Ir-Re interfaces were found in a similar manner. For this testing, the outer wall emissivity was assumed to be 0.8, a good assumption for the high emissivity, dendritic Re outer wall. The ambient temperature was assumed to be 278 K, which was generally consistent with measurements of the test tank inner walls. The most questionable assumptions made in the temperature estimates were the thermal conductivities of the ceramic oxides, where there is some variance in the reported values. For this study, the thermal conductivities of the layers were taken from reference 8. The inner layer of the Phase I chamber was assumed to have the thermal conductivity of  $ZrO_2$ , although the coating was infiltrated with sol gel  $HfO_2$ .

The two-color pyrometer measurements for each chamber are plotted against mixture ratio in figure 4. The maximum operating temperature for all of the chambers was at stoichiometric mixture ratio. The outer wall temperatures at mixture ratio 8 ranged from 1845 °C for the thick-walled  $HfO_2$  (7731-4-9) chamber to 2315 °C for the thin-walled  $ZrO_2$  (Phase I) chamber. The temperature drop through the wall and through the oxide layer for each of the chambers, at mixture ratio 8, is shown in figure 5. For all of the chambers, the overwhelming majority of the temperature drops through the walls were caused by the oxide layer, which has thermal conductivities two orders of magnitude lower than Ir. The temperature drop through the  $ZrO_2$  layers ranged from 213 °C for the 17-mil-thick chamber (7731-4-1) to 284 °C for the 34-mil-thick chamber (7731-4-4). The 33-mil-thick  $HfO_2$  chamber (7731-4-9) provided a temperature drop of 574 °C. The Ir layer never provided more than a 2 °C temperature drop. The large thermal resistance of the oxide layer resulted in a significantly reduced temperature at the Ir surface and at the Ir-Re interface.

The Ir-Re rocket life model from reference 4 (accounting only for diffusion) showed chamber life has an exponential dependence on temperature. The effect of reducing temperature at the Ir surface would be more pronounced at lower operating temperatures. For example, a reduction from 1800 to 1600 °C at the Ir surface is predicted to give 40 more hours of operating life before 20 percent Re concentration is reached. A reduction from 2200 to 2000 °C, however, would give 9 more hours of lifetime before 20 percent Re concentration is reached.

## POSTTEST INSPECTION

### Sectioning of Chambers

Electrical discharge machining (EDM) has proven to be the most effective way to section Ir-Re engines, but the ceramic coatings are not conductive, which is necessary for EDM. However, the 6063-1-10 chamber had a sufficiently thin ceramic coating that it was still able to be sectioned lengthwise by EDM. This was not possible for the five chambers with the thick, monolithic coatings. The 7731-4-3, 7731-4-9, and 7731-4-12 chambers were potted with an epoxy and sectioned lengthwise by using an alumina cutting wheel. The epoxy was then melted out, although some epoxy residue remained in the cracks. The 7731-4-4 chamber was mistakenly sectioned by an alumina cutting wheel without the potting material and lost most of its ceramic coating as a result. The Phase I and 7731-4-1 chambers were sectioned by Ultramet with laser machining.

### Visual Inspection

Thick-walled chambers.—The five chambers with monolithic oxide coatings had visible macrocracks in their coatings down the length of the chambers on the first inspection (6 firings at mixture ratio 4). In general the cracking was more extensive in the thicker coated (>30 mils) chambers, which were subject to larger temperature gradients through the oxide layer. Despite the cracking, there was no evidence of any spalling or chipping of the oxide coatings through all of the testing up to mixture ratio 8 (minimum of 14 firings). In the high mixture ratio testing, however, chipping of the coating began to occur in both of the  $\text{HfO}_2$ -coated chambers (7731-4-9 and 7731-4-12) and the thicker coated  $\text{ZrO}_2$  chambers (7731-4-3 and 7731-4-4). The chipping occurred at the head end of the chambers, just downstream of where the attachment cone transitioned into the barrel section. This region is an area of relatively high stress, since the attachment cone is mechanically torqued down onto the water-cooled section and has high thermal gradients because of the proximity to the water cooling. The chipping appeared to occur within the oxide layer, because there was some of the oxide layer left. Given that it occurred most at a stress concentrator, the chipping in these chambers was probably due to repeated thermal cycling rather than operation at high mixture ratio. The 7731-4-4 chamber lost its 32-mil-thick  $\text{ZrO}_2$  coating entirely, from the throat to the nozzle exit. There were occasional chips of the oxide layer removed down the length of the barrel section of the 7731-4-1 chamber.

Despite extensive macrocracking in these chambers, the Ir layer appeared to be attacked by oxidation only in those places where the oxide coating was removed outright (ref. 8). This would indicate that the ceramic oxide layer compressed during firing and sealed the cracks in the layer, which protected the underlying Ir. Upon cooling of the chamber, the oxide layer would expand, thereby causing cracking in the coating once more. The cracks would perhaps be larger and more extensive in the hotter regions of the chamber. Such repeated compression and expansion of the brittle ceramic oxides would lead to the eventual spalling of the coating. However, since most of the chipping occurred within the oxide layer rather than at the oxide-Ir interface, a strong bond between the oxide and Ir layers was indicated. Furthermore, most of the chipping occurred at a stress concentrator particular to the testing apparatus. A chamber welded directly to the injector (eliminating the attachment cone) may be capable of more thermal cycles than what was demonstrated in this test series. The exception to this line of reasoning is the chamber (7731-4-4) in which the entire oxide layer spalled off at the throat. The adhesion between the Ir and oxide layers in this chamber was not sufficient to withstand repeated thermal cycling, at least at the throat.

Thin-walled chambers.—Inspection of the thin-walled  $\text{ZrO}_2$  chamber (Phase I) and the composite chamber (6063-1-10) throughout the test program found no evidence of the visible macrocracking



experienced by the five thick-walled chambers. The thin-walled chambers, however, suffered burn-throughs during high mixture ratio tests. For both chambers, the burn-throughs occurred in the converging section, just upstream of the throat. Figure 6 shows the burn-through for the composite chamber. It was determined that the integrity of the exterior purge was maintained during both burn-throughs, so that the burn-throughs are felt to have occurred from the inside-out. The  $\text{ZrO}_2$  chamber failed during its 7th mixture ratio 11 test, whereas the composite chamber failed during its 30th mixture ratio 16 test. For both chambers there was no evidence of imminent failure from the last visual inspection before failure. The composite chamber suffered a second burn-through in the barrel section of the chamber, close to the front end of the chamber. From videotape replay of the test, it was apparent that this second burn-through occurred after the one in the converging section.

The Phase I chamber was sent to Ultramet, whereas the sectioned 6063-1-10 chamber was examined under a microscope. Microcracking of the coating that was not apparent from visual inspection of the chamber was found. Considering the amount of time these chambers were operated in a high mixture ratio environment, these small cracks apparently resealed during firing. Examination of the burn-through showed that a large volume of the Ir and Re layers was removed around the smaller hole in the burn-through (fig. 6). There are regions down the length of the chamber where part of the Ir and Re layers had been removed, whereas the inner oxide coating was largely intact. The thinness of the coatings could be responsible for this behavior. The thin coatings would provide for more rapid diffusion (for both  $\text{O}_2$  and Ir oxidation products) through the oxide layer and higher temperatures at the Ir surface. The diffusion through the coating would be accelerated by operation in the severely oxidizing environment of mixture ratio 16  $\text{GH}_2/\text{GO}_2$ .

## SUMMARY OF RESULTS

Ceramic oxide coatings, such as zirconia ( $\text{ZrO}_2$ ) or hafnia ( $\text{HfO}_2$ ), can serve as a thermal and a diffusion barrier for iridium-rhenium (Ir-Re) chambers, reducing the temperature and partial pressure of oxygen ( $\text{O}_2$ ) at the Ir surface. The synergistic effects of the oxide coatings could result in significantly longer life operation for Ir-Re rockets, as well as operation in highly oxidizing environments. Seven ceramic oxide-coated Ir-Re, 22-N class chambers were tested on gaseous hydrogen/gaseous oxygen ( $\text{GH}_2/\text{GO}_2$ ) propellants. All of the coatings survived the thermal shock of combustion and demonstrated operation in aggressively oxidizing environments.

Five of the chambers had monolithic coatings of either  $\text{ZrO}_2$  or  $\text{HfO}_2$  of thicknesses ranging from 11 mils to 34 mils. The oxide coatings compressed during firing and expanded during cool down; this resulted in extensive macrocracking in the oxide layer. After a minimum of 14 firings and 25 minutes at mixture ratios from 4 to 8, there was no evidence of chipping or spalling of the coatings. The cracks apparently resealed under compression of the layer during firing, thereby protecting the underlying Ir layer. The coatings in these chambers did begin to chip upon further testing at mixture ratio 11. The chipping of the oxide layer generally occurred near the attachment cone (a probable stress concentrator for this testing apparatus) and was probably the result of repeated thermal cycling rather than operation at a high mixture ratio. The chipping occurred within the oxide layer rather than at the Ir-oxide interface, thus indicating a strong bond between the Ir and oxide layers. However, one chamber did lose its entire oxide coating, downstream from the throat to the nozzle exit.

A chamber with a 1-mil  $\text{ZrO}_2$  layer infiltrated with sol gel  $\text{HfO}_2$  and another chamber with a thin composite Ir-oxide layer were also tested. These chambers did not experience the macrocracking of the chambers with the monolithic coatings, but did suffer burn-throughs in the throat region after extensive testing. The thin  $\text{ZrO}_2$ -coated chamber was tested for 25 firings and approximately 28 minutes at mixture

ratios 4 to 11. The composite coated chamber was tested for 48 firings and over 52 minutes at mixture ratios 4 to 16 (including 30 firings and over 29 minutes at mixture ratio 16). With both thin-walled chambers, the erosion of the underlying Ir and Re layers was more extensive than that of the oxide layer. This likely occurred because of the diffusion of oxidizers and Ir oxidation products through the thin oxide layers, accelerated by operation in the severely oxidizing environment of high mixture ratio  $\text{GH}_2/\text{GO}_2$ .

In all of the chambers, the oxide layer provided most of the temperature drop through the wall. The thicker coated chambers provided the larger temperature drops through the oxide layer, with the 33-mil-thick  $\text{HfO}_2$  chamber providing the largest (570 °C). The large thermal resistance of the oxide layer resulted in significantly reduced temperatures at the Ir surface and at the Ir-Re interface, slowing the temperature-dependent processes of Ir oxidation and Re diffusion into Ir.

The results of this test program indicated that the thin-walled coatings are better suited for repeated thermal cycling than the thick-walled coatings, particularly in low oxidizing environments such as Earth-storable or low mixture ratio  $\text{GH}_2/\text{GO}_2$  propellants. However, the thin oxide coatings were more susceptible to burn-throughs in high mixture ratio  $\text{GH}_2/\text{GO}_2$ . Thicker oxide coatings may be required for operating in high oxidizing environments, although the coatings will be more susceptible to cracking after repeated thermal cycling.

#### REFERENCES

1. Schoenman, L.: 4000 °F Materials For Low Thrust Rocket Engines, AIAA Paper 93-2406, June 1993.
2. Schneider, S.J.: High Temperature Thruster Technology for Spacecraft Propulsion, IAF Paper 91-254, October 1991.
3. Wooten, J.R.; and Lansaw, P.T.: High-Temperature, Oxidation-Resistant Thruster Research, Final Report, Contract NAS3-24643, NASA CR-185233, February 1990.
4. Hamilton, J.C., et. al.: Diffusion Mechanisms in Iridium-Coated Rhenium for High-Temperature, Radiation-Cooled Rocket Thrusters, AIAA Paper 91-2215, June 1991.
5. Wood, R.: Experiences With High Temperature Materials For Small Thrusters, AIAA Paper 93-1963, June 1993.
6. Tuffias, R.H., et. al.: Enhanced Oxidation Protection For Iridium-Lined Rhenium Thrust Chambers, Final Report, Contract NAS3-25468, June 1990.
7. Tuffias, R.H.: Protective Oxide Coatings for Iridium/Rhenium Chambers, Final Report, Contract NAS3-26253.
8. Tuffias, R.H., et. al.: Design, Analysis, and Fabrication of Oxide-Coated Iridium/Rhenium Combustion Chambers, presented at the 1993 JANNAF Propulsion Meeting, November 1993 (to be published in meeting proceedings).
9. Arrington, L.A.; and Schneider, S.J.: Low Thrust Rocket Test Facility, AIAA Paper 90-2503, NASA TM-103206, July 1990.
10. Fluid Meters: Their Theory and Application, American Society of Mechanical Engineers, 1971.

11. Handbook For Estimating the Uncertainty in Measurements Made With Liquid Propellant Rocket Engine Systems, Chemical Propulsion Information Agency Document Number 180, April 1969.
12. Gordon, S.; and McBride, B.: Computer Program for Calculation of Complex Chemical Equilibrium Composition, Rocket Performance, Incident and Reflected Shocks, and Chapman-Jouguet Detonations, NASA SP-273, March 1976.
13. Gerhardt, D.L.: Integrated Hydrogen/Oxygen Technology Applied to Auxiliary Propulsion Systems, Final Report, Contract NAS3-25643, NASA CR-185289, September 1990.

Table I.—Ceramic Oxide-Coated Iridium-Rhenium Chambers

Chamber	Structure
Phase I	1 mil $\text{ZrO}_2$ infiltrated with sol gel $\text{HfO}_2$ /4 mils Ir/41 mils Re
7731-4-1	17 mils $\text{ZrO}_2$ /2 mils Ir/68 mils Re
7731-4-3	34 mils $\text{ZrO}_2$ /1 mil Ir/73 mils Re
7731-4-4	32 mils $\text{ZrO}_2$ /2 mils Ir/61 mils Re
7731-4-9	33 mils $\text{HfO}_2$ /2 mils Ir/51 mils Re
7731-4-12	11 mils $\text{HfO}_2$ /2 mils Ir/56 mils Re
6063-1-10	Ir-Oxide composite (proprietary)/2 mils Ir/69 mils Re

Table II.—Test Results

Chamber	Number of firings	Time, sec	Mixture ratio range	Wall temperature, °C		Comments
				Outer wall maximum	Inner wall estimate	
Phase I	25	1665	4 to 11	2316	2333	No macrocracking of the oxide layer occurred; a burn-through occurred in the throat region on the seventh mixture ratio 11 test
7731-4-1	24	1942	4 to 11	2233	2524	Macrocracking of the oxide layer early; after high mixture ratio testing, some chipping of the oxide layer occurred
7731-4-3	18	1470	4 to 11	2074	2488	Extensive macrocracking of the oxide layer early; some chipping of the oxide, near the attachment cone, began to occur in the high mixture ratio testing
7731-4-4	23	1812	4 to 11	2010	2341	Extensive macrocracking of the oxide layer early; some chipping of the oxide, near the attachment cone, began to occur in the high mixture ratio testing; during the final test, the entire oxide layer, downstream from the throat to the nozzle exit, was lost
7731-4-9	24	1931	4 to 11	1895	2501	Extensive macrocracking of the oxide layer early; some chipping of the oxide, near the attachment cone, began to occur in the high mixture ratio testing
7731-4-12	27	1933	4 to 11	2142	2498	Extensive macrocracking of the oxide layer early; some chipping and spalling of the oxide, near the attachment cone, began to occur in the high mixture ratio testing
6063-1-10	48	3141	4 to 16	2207	2427	Testing included 30 firings for 1753 sec at mixture ratio 16; no macrocracking of the coating, but burn-throughs in the converging section and in the head end region occurred on the final mixture ratio 16 test; the burn-through in the converging section occurred before the one in the head end region

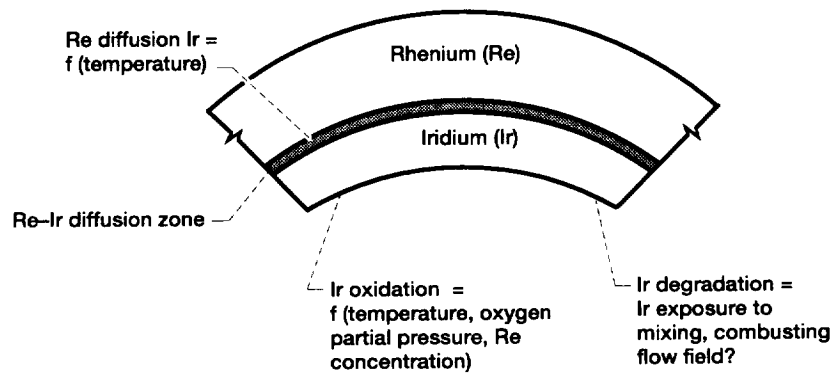


Figure 1.—Life-limiting mechanisms for iridium-rhenium rockets.

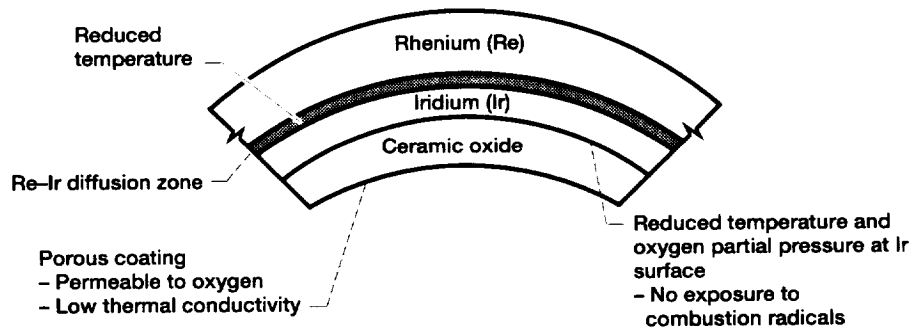
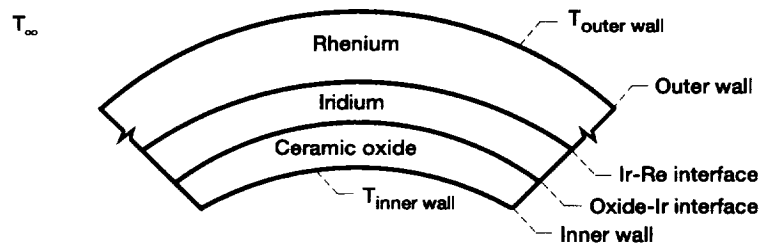


Figure 2.—Effect of ceramic-oxide coatings on iridium-rhenium rockets.



At outer surface:

$$q_{\text{radiation}} = q_{\text{conduction}}$$

$$q_{\text{radiation}} = (2\pi R_{\text{outer}} L) \epsilon_{\text{outer}} \sigma (T_{\text{outer}}^4 - T_{\infty}^4)$$

$$q_{\text{conduction}} = \frac{T_{\text{inner}} - T_{\text{outer}}}{\frac{\ln(R_{\text{outer}}/R_{\text{Ir-Re}})}{2\pi K_{\text{Re}} L} + \frac{\ln(R_{\text{Ir-Re}}/R_{\text{Ox-Ir}})}{2\pi K_{\text{Ir}} L} + \frac{\ln(R_{\text{Ox-Ir}}/R_{\text{inner}})}{2\pi K_{\text{Ox}} L}}$$

Therefore:

$$T_{\text{inner}} = T_{\text{outer}} + [R_{\text{outer}} \epsilon_{\text{outer}} \sigma (T_{\text{outer}}^4 - T_{\infty}^4)] \times$$

$$\frac{\ln(R_{\text{outer}}/R_{\text{Ir-Re}})}{K_{\text{Re}}} + \frac{\ln(R_{\text{Ir-Re}}/R_{\text{Ox-Ir}})}{K_{\text{Ir}}} + \frac{\ln(R_{\text{Ox-Ir}}/R_{\text{inner}})}{K_{\text{Ox}}}$$

T = temperature

R = radius

L = length

K = thermal conductivity

q = heat rate

$\epsilon$  = emissivity

$\sigma$  = Stefan-Boltzmann constant

Figure 3.—Methodology for determining wall temperature profile.

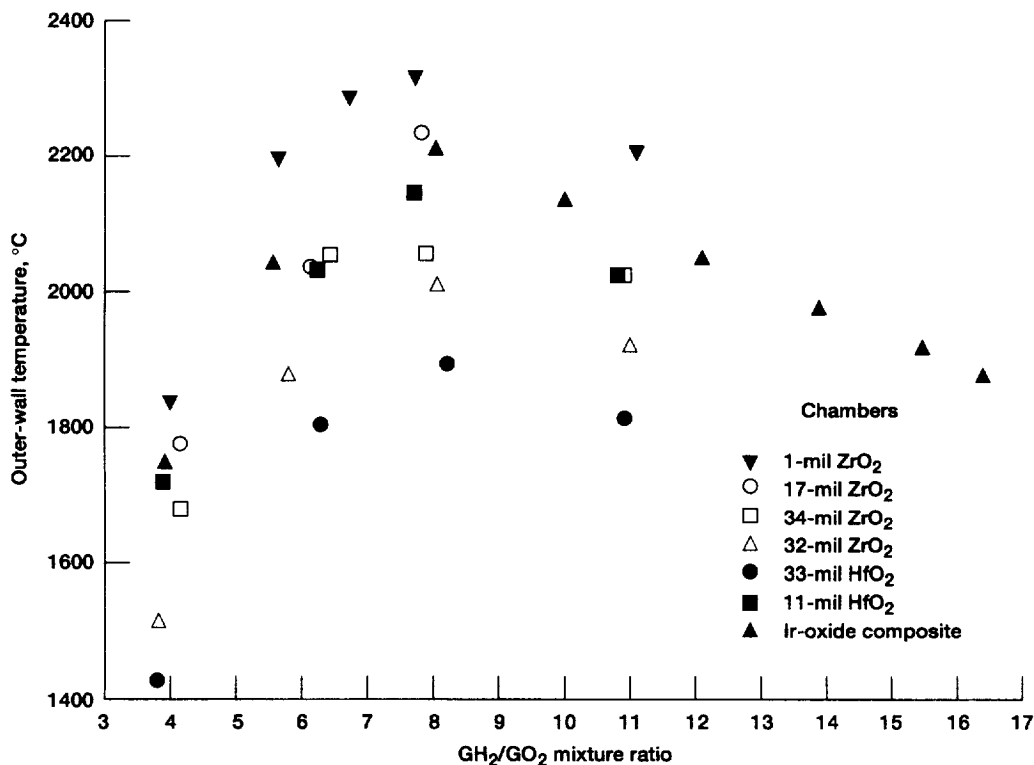


Figure 4.—Two-color pyrometer measurements versus mixture ratio.

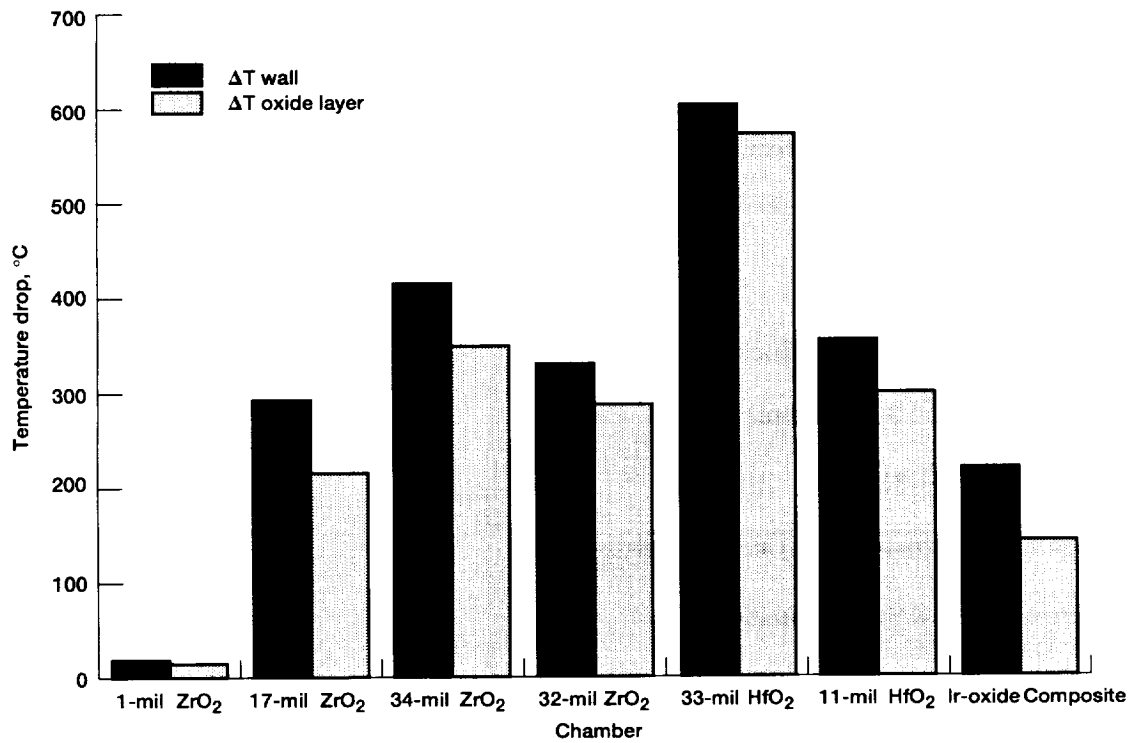


Figure 5.—Estimated temperature drop through chamber wall and oxide layer at mixture ratio = 8 with assumed emissivity = 0.8.



Figure 6.—Chamber 6063-1-10 (iridium-oxide composite coating) throat region exterior.

REPORT DOCUMENTATION PAGE			Form Approved OMB No. 0704-0188	
Public reporting burden for this collection of information is estimated to average 1 hour per response, including the time for reviewing instructions, searching existing data sources, gathering and maintaining the data needed, and completing and reviewing the collection of information. Send comments regarding this burden estimate or any other aspect of this collection of information, including suggestions for reducing this burden, to Washington Headquarters Services, Directorate for Information Operations and Reports, 1215 Jefferson Davis Highway, Suite 1204, Arlington, VA 22202-4302, and to the Office of Management and Budget, Paperwork Reduction Project (0704-0188), Washington, DC 20503.				
1. AGENCY USE ONLY (Leave blank)		2. REPORT DATE March 1994		3. REPORT TYPE AND DATES COVERED Technical Memorandum
4. TITLE AND SUBTITLE  Evaluation of Oxide-Coated Iridium-Rhenium Chambers			5. FUNDING NUMBERS  WU-506-42-31	
6. AUTHOR(S)  Brian D. Reed				
7. PERFORMING ORGANIZATION NAME(S) AND ADDRESS(ES)  National Aeronautics and Space Administration Lewis Research Center Cleveland, Ohio 44135-3191			8. PERFORMING ORGANIZATION REPORT NUMBER  E-8286	
9. SPONSORING/MONITORING AGENCY NAME(S) AND ADDRESS(ES)  National Aeronautics and Space Administration Washington, D.C. 20546-0001			10. SPONSORING/MONITORING AGENCY REPORT NUMBER  NASA TM-106442	
11. SUPPLEMENTARY NOTES Prepared for the 1993 JANNAF Propulsion Meeting, sponsored by the JANNAF Interagency Propulsion Committee, Monterey, California, November 15-19, 1993. Responsible person, Brian R. Reed, organization code 5330, (216)977-7489.				
12a. DISTRIBUTION/AVAILABILITY STATEMENT  Unclassified - Unlimited Subject Category 20			12b. DISTRIBUTION CODE	
13. ABSTRACT (Maximum 200 words)  Iridium-coated rhenium (Ir-Re) provides long life operation of radiation-cooled rockets at temperatures up to 2200 °C. Ceramic oxide coatings could be used to increase Ir-Re rocket lifetimes and allow operation in highly oxidizing environments. Ceramic oxide coatings promise to serve as both thermal and diffusion barriers for the iridium layer. Seven ceramic oxide-coated Ir-Re, 22-N rocket chambers were tested with gaseous hydrogen/gaseous oxygen (GH <sub>2</sub> /GO <sub>2</sub> ) propellants. Five chambers had thick (over 10 mils), monolithic coatings of either hafnia (HfO <sub>2</sub> ) or zirconia (ZrO <sub>2</sub> ). Two chambers had coatings with thicknesses less than 5 mils. One of these chambers had a thin-walled coating of ZrO <sub>2</sub> infiltrated with sol gel HfO <sub>2</sub> . The other chamber had a coating composed of an Ir-oxide composite. The purpose of this test program was to assess the ability of the oxide coatings to withstand the thermal shock of combustion initiation, adhere under repeated thermal cycling, and operate in aggressively oxidizing environments. All of the coatings survived the thermal shock of combustion and demonstrated operation at mixture ratios up to 11. Testing the Ir-oxide composite-coated chamber included over 29 min at mixture ratio 16. The thicker walled coatings provided the larger temperature drops across the oxide layer (up to 570 °C), but were susceptible to macrocracking and eventual chipping at a stress concentrator. The cracks apparently resealed during firing, under compression of the oxide layer. The thinner walled coatings did not experience the macrocracking and chipping of the chambers that was seen with the thick, monolithic coatings. However, burn-throughs in the throat region did occur in both of the thin-walled chambers at mixture ratios well above stoichiometric. The burn-throughs were probably the result of oxygen diffusion through the oxide coating that allowed the underlying Ir and Re layers to be oxidized. The results of this test program indicated that the thin-walled oxide coatings are better suited for repeated thermal cycling than the thick-walled coating, while thicker coatings may be required for operation in aggressively oxidizing environments.				
14. SUBJECT TERMS  Radiation-cooled engines; Iridium; Rhenium; Zirconia; Hafnia; Oxide coatings			15. NUMBER OF PAGES 15	
			16. PRICE CODE A03	
17. SECURITY CLASSIFICATION OF REPORT Unclassified	18. SECURITY CLASSIFICATION OF THIS PAGE Unclassified	19. SECURITY CLASSIFICATION OF ABSTRACT Unclassified	20. LIMITATION OF ABSTRACT	